Coupled buoyancy and thermocapillary convection in a viscoelastic Maxwell fluid

1993 J. Phys.: Condens. Matter 5 4343

(http://iopscience.iop.org/0953-8984/5/26/007)

J. Phys.: Condens. Matter 5 (1993) 4343–4352. Printed in the UK

Coupled buoyancy and thermocapillary convection in a viscoelastic Maxwell fluid

P C Dauby†, P Parmentier†, G Lebon† and M Grmela‡

† Institut de Physique B5, Université de Liège, Sart Tilman, B-4000 Liège, Belgium
‡ École Polytechnique de Montréal, Montréal, H3C 3A7, Canada

Received 4 January 1993, in final form 5 April 1993

Abstract. Linear coupled buoyancy and thermocapillary instabilities (the Bénard–Marangoni problem) in a Maxwell viscoelastic fluid layer heated from below are studied. As the principle of exchange of stability is no longer valid, both stationary and oscillatory solutions are considered. It is shown that beyond a critical value of the relaxation time, the instability appearing in a fluid layer with a free upper surface subject to a temperature-dependent surface tension takes the form of oscillations. The critical temperature difference between the lower and upper surfaces is determined as a function of the Prandtl number and the relaxation time. The instability thresholds are graphically represented on 'Nield's diagrams' where the critical Marangoni number is given versus the Rayleigh number. At high Prandtl numbers discontinuities in the solutions are displayed for some specific values of the fluid layer thickness. It is also observed that for some range of variation of the parameters, thermocapillarity has an unusual stabilizing effect.

1. Introduction

The problem of thermoconvection in Newtonian fluids has been studied for many years; fairly complete linear and non-linear results are now available for both gravity-(Rayleigh–Bénard) and thermocapillarity-(Marangoni) driven convection. Classical references about this subject are listed as [1]–[16].

However it is nowadays well known [17–20] that a wide class of real fluids such as polymeric solutions are actually viscoelastic. Thermoconvection in polymeric liquids has drawn much less interest than that in Newtonian fluids. Except for rare works [21, 22], the analyses are only linear [23–25]. Moreover in most cases, the single motor of instability taken into account is gravity. To our knowledge, thermocapillary instability in a non-Newtonian fluid has only been studied by Getachew and Rosenblat [26] and Lebon and Cloot [27].

The purpose of the present paper is to study the onset of convection in a horizontal thin layer of a viscoelastic fluid at rest and heated from below under the simultaneous actions of gravity and thermocapillarity (the Bénard–Marangoni problem). The analysis is linear and must thus be regarded as a first step towards a more general non-linear approach. The rheology of the fluid is assumed to be described by the Maxwell viscoelastic model.

The paper will be organized as follows. In section 2, the governing equations are briefly derived. Section 3 is devoted to the numerical method used to solve the equations. Results are discussed in section 4 and final conclusions are drawn in section 5.

0953-8984/93/264343+10$07.50

2. The mathematical formulation

Consider a viscoelastic incompressible fluid layer of infinite horizontal extent and thickness d. The layer is confined between a lower perfectly heat conducting boundary and an upper free surface adiabatically isolated. The surface tension ξ is assumed to depend linearly on the temperature T:

$$\xi = \xi_0 - \gamma(T - T_0) \tag{2.1}$$

where ξ_0 is the surface tension at the reference temperature T_0, and γ is assumed to be a constant which is positive for most current liquids and is of the order of magnitude of 10^{-1} Pa.

The constitutive equation giving the dependence of the viscous stress tensor τ with respect to the velocity gradient tensor ∇u is the well known Maxwell equation [17–20]:

$$\tau + \lambda_1 \partial\tau/\partial t = \mu[\nabla u + (\nabla u)^T] \tag{2.2}$$

where λ_1 is the relaxation time and μ is the dynamic viscosity; μ and λ_1 are positive quantities [17] with λ_1 ranging from 10^{-12} s for water to 10^2 s for some rheological fluids [18].

For convenience, the variables are expressed in dimensionless form. Lengths are scaled by the thickness d of the layer; the velocity u, time t, pressure p, stress tensor τ, temperature differences and surface tension are scaled by κ/d, d^2/κ, $\kappa\mu/d^2$, $\kappa\mu/d^2$, βd and ξ_0 respectively; κ is the heat diffusivity while $\beta = \Delta T/d$ is the modulus of the temperature gradient between the bottom and the top of the layer; β is positive for a fluid layer heated from below. The following dimensionless numbers are also introduced:

$$\mathrm{Pr} \equiv \mu/\rho_0\kappa \tag{2.3}$$

$$\mathrm{Ma} \equiv \gamma\beta d^2/\kappa\mu \tag{2.4}$$

$$\mathrm{Ra} \equiv \rho_0 g\alpha\beta d^4/\kappa\mu \tag{2.5}$$

$$\lambda \equiv \lambda_1\kappa/d^2 \tag{2.6}$$

where Pr is the Prandtl number, Ra the Rayleigh number, Ma the Marangoni number, ρ_0 the density at temperature T_0, g the gravity acceleration, α is the thermal expansion coefficient (considered positive here) and λ is the dimensionless relaxation time λ_1. As γ is usually larger than zero, Ma is supposed to be positive.

Within Boussinesq's approximation, the governing dimensionless balance equations of mass, momentum and energy are

$$\nabla \cdot u = 0 \tag{2.7}$$

$$\partial u/\partial t + u \cdot \nabla u = \mathrm{Pr}(-\nabla p + \mathrm{Ra}\, e_z + \nabla \cdot \tau) \tag{2.8}$$

$$\partial T/\partial t + u \cdot \nabla T = \nabla^2 T \tag{2.9}$$

where e_z is the vertical unit vector whose direction is opposite to gravity.

If the plane $z = 0$ is located at half height of the fluid layer, the solution describing pure conduction is given by $u^c = 0$ and $T^c = T_{\mathrm{bottom}} - \beta(z + \frac{1}{2})$. Using (2.2) and (2.7)–(2.9) it is

an easy task to eliminate the pressure p, the horizontal components u and v of the velocity and the viscous stress tensor τ; one obtains in this way the following linear equations for the perturbations with respect to the conductive solution:

$$[\nabla^2 - (1 + \lambda\partial/\partial t)\mathrm{Pr}^{-1}\partial/\partial t]\nabla^2 w = -(1 + \lambda\partial/\partial t)\mathrm{Ra}\nabla_h^2\theta \tag{2.10}$$

$$\partial\theta/\partial t - w = \nabla^2\theta \tag{2.11}$$

where the quantity θ is defined by $\theta = T - T^c$, w is the vertical velocity component and ∇_h is the horizontal nabla operator ($\nabla_h^2 = \partial^2/\partial x^2 + \partial^2/\partial y^2$).

The corresponding boundary conditions are

$$w = \mathrm{D}w = \theta = 0 \qquad \text{at} \qquad z = -\tfrac{1}{2} \tag{2.12}$$

$$w = 0 \qquad \mathrm{D}^2 w - \mathrm{Ma}(1 + \lambda\partial/\partial t)\nabla_h^2\theta = 0 \qquad \mathrm{D}\theta = 0 \qquad \text{at} \qquad z = \tfrac{1}{2} \tag{2.13a–c}$$

where D stands for d/dz. The first two equations in (2.12) express the no-slip condition on a rigid surface while the third one expresses the fixed temperature condition. Equation (2.13*a*) takes account of the non-deformability of the surface, (2.13*b*) is the Marangoni condition expressing that the shear effect at the upper surface is balanced by the gradient of surface tension and finally (2.13*c*) is the adiabaticity condition.

According to the normal mode technique, we seek solutions of the form

$$(w, \theta) = [W(z), \Theta(z)]\exp[\mathrm{i}(k_x x + k_y y) + \sigma t] \tag{2.14}$$

where k_x and k_y are the x and y components of the disturbance wave vector k; σ is the complex stability parameter

$$\sigma = \sigma_r + \mathrm{i}\omega \tag{2.15}$$

where σ_r measures the growth rate of the disturbance and ω its frequency. Substitution of (2.15) in (2.10–12) results in the following differential equations and boundary conditions for the disturbance amplitudes $W(z)$ and $\Theta(z)$:

$$(\mathrm{D}^2 - k^2)^2 W - (1 + \lambda\sigma)\mathrm{Pr}^{-1}\sigma(\mathrm{D}^2 - k^2)W = \mathrm{Ra}\,k^2(1 + \lambda\sigma)\Theta \tag{2.16}$$

$$(\mathrm{D}^2 - k^2 - \sigma)\Theta + W = 0 \tag{2.17}$$

and

$$W(-\tfrac{1}{2}) = \mathrm{D}W(-\tfrac{1}{2}) = \Theta(-\tfrac{1}{2}) = 0 \tag{2.18}$$

$$W(\tfrac{1}{2}) = \mathrm{D}^2 W(\tfrac{1}{2}) + \mathrm{Ma}\,k^2(1 + \lambda\sigma)\Theta(\tfrac{1}{2}) = \mathrm{D}\Theta(\tfrac{1}{2}) = 0 \tag{2.19}$$

where $k = \sqrt{k_x^2 + k_y^2}$. Note that for $\sigma_r = \omega = 0$ (exchange of stability), the set (2.16–19) is independent of the relaxation time λ.

3. The numerical procedure

The system (2.16–17) and boundary conditions (2.18–19) can be written in the standard form of a first-order set of six linear and homogeneous differential equations:

$$\mathrm{D}x = \mathbf{A}x \tag{3.1}$$

with linear and homogeneous boundary conditions

$$\mathbf{B}x(-\tfrac{1}{2}) + \mathbf{C}x(\tfrac{1}{2}) = 0 \tag{3.2}$$

In (3.1–2) the following notation is used:

$$x^T = [W, DW, D^2W, D^3W, \Theta, D\Theta] \tag{3.3}$$

$$\mathbf{A} = \begin{bmatrix} 0 & 1 & 0 & 0 & 0 & 0 \\ 0 & 0 & 1 & 0 & 0 & 0 \\ 0 & 0 & 0 & 1 & 0 & 0 \\ -k^2(k^2 + \mathrm{Pr}^{-1}\sigma\phi) & 0 & 2k^2 + \sigma\phi & 0 & k^2\mathrm{Ra} + \mathrm{Pr}^{-1}\sigma\phi & 0 \\ 0 & 0 & 0 & 0 & 0 & 1 \\ -1 & 0 & 0 & 0 & k^2 + \sigma & 0 \end{bmatrix} \tag{3.4}$$

$$\mathbf{B} = \begin{bmatrix} 1 & 0 & 0 & 0 & 0 & 0 \\ 0 & 1 & 0 & 0 & 0 & 0 \\ 0 & 0 & 0 & 0 & 1 & 0 \\ 0 & 0 & 0 & 0 & 0 & 0 \\ 0 & 0 & 0 & 0 & 0 & 0 \\ 0 & 0 & 0 & 0 & 0 & 0 \end{bmatrix} \qquad \mathbf{C} = \begin{bmatrix} 0 & 0 & 0 & 0 & 0 & 0 \\ 0 & 0 & 0 & 0 & 0 & 0 \\ 0 & 0 & 0 & 0 & 0 & 0 \\ 1 & 0 & 0 & 0 & 0 & 0 \\ 0 & 1 & 0 & 0 & 0 & 0 \\ 0 & 0 & 1 & 0 & k^2\mathrm{Ma}\phi & 0 \end{bmatrix} \tag{3.5}$$

with $\phi = 1 + \lambda\sigma$. Note that the quantities **A**, **B** and **C** are independent of z.

The solution of the set (3.1) may be formally written as

$$x = \exp(\mathbf{A}z)x(0). \tag{3.6}$$

Introducing this expression in the boundary conditions (3.2) yields

$$[\mathbf{B}\exp(-\mathbf{A}/2) + \mathbf{C}\exp(\mathbf{A}/2)]x(0) = 0. \tag{3.7}$$

Non-trivial solutions for (3.6) exist if the following relation is satisfied:

$$det[\mathbf{B}\,exp(-\mathbf{A}/2) + \mathbf{C}\,exp(\mathbf{A}/2)] = 0. \tag{3.8}$$

This condition may also be viewed as a linear equation for the Marangoni number

$$f_1(k, \sigma, \mathrm{Ra}, \mathrm{Pr}, \lambda) + \mathrm{Ma}\,f_2(k, \sigma, \mathrm{Ra}, \mathrm{Pr}, \lambda) = 0 \tag{3.9}$$

where f_1 and f_2 are complex functions depending on the whole set of parameters. The functions f_1 and f_2 become real for $\sigma = 0$.

Relation (3.9) is the complex eigenvalue equation which allows for the determination of the marginal stability threshold.

The expression $\exp(-\mathbf{A}/2)$ is numerically evaluated by the series expansion

$$\exp(-\mathbf{A}/2) \simeq \mathbf{I} + (-\mathbf{A}/2) + (-\mathbf{A}/2)^2/2! + \cdots + (-\mathbf{A}/2)^n/n! \tag{3.10}$$

while $\exp(\mathbf{A}/2)$ is calculated by inverting $\exp(-\mathbf{A}/2)$: $\exp(\mathbf{A}/2) = [\exp(-\mathbf{A}/2)]^{-1}$.

Solutions of (3.9) are obtained from a Newton–Raphson algorithm for a (2×2) non-linear real system. The minimization of Ra or Ma with respect to k is also realized by a Newton–Raphson algorithm applied to the equation $\partial\mathrm{Ra}/\partial k = 0$ or $\partial\mathrm{Ma}/\partial k = 0$, with numerical evaluations of the first and second derivatives. The computations are performed on a 6000/550 RISK IBM station.

4. Results and discussion

The loss of linear stability is characterized by the vanishing of σ_r, the real part of the stability parameter σ. When the frequency ω is zero, the instability is stationary, otherwise it is oscillatory. In the case of a Newtonian fluid the principle of exchange of stability has been shown [28, 29], which means that the instability is always stationary. For a Maxwell fluid this principle no longer holds and the two kinds of instability must be examined.

The description of the stationary instability is directly carried out since in this case equations (2.16)–(2.19) reduce to those of Nield [7] for a Newtonian fluid.

New interesting phenomena are observed when oscillatory convection sets in.

Typical marginal stability curves Ma(k) are given in figures 1 and 2. The full curve represents the stationary neutral curves ($\omega = 0$); it depends only on the Rayleigh number Ra, not on the Prandtl number Pr or on the viscoelastic relaxation time λ. Broken curves describe overstability ($\omega \neq 0$) and are functions of Ra, Pr and λ. The minima of the curves Ma(k) give the critical Marangoni numbers and the critical wave-numbers.

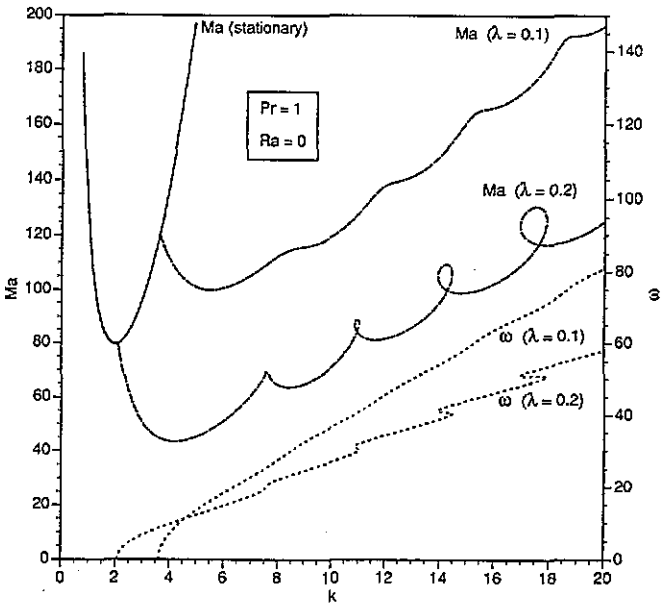

Figure 1. Neutral curves Ma(k) and $\omega(k)$ for Pr = 1 and Ra = 0 and for two values λ = 0.1 and 0.2 of the relaxation time. The full (broken) curve corresponds to stationary (oscillatory) instability.

Figure 1 shows the Marangoni number Ma and the frequency ω of the oscillations versus the wave-number for Ra = 0, Pr = 1 and two values of the relaxation time λ. The loops in the overstability curves describe mathematical solutions which are not important from a physical point of view since only the lower envelope is relevant for the appearance of convection. However it is interesting to notice that even if the Marangoni number is continuous along this lower envelope, this is no longer true for the frequency ω. This feature—and thus the presence of loops in the marginal curves—could be observed in experiments by imposing the value of the wave-number.

Figure 2 reproduces the marginal stability curves for different values of the Prandtl and Rayleigh numbers. For clarity, the loops have been dropped and only the lower envelopes are plotted. The presence of a second marginal curve with negative concavity for Pr = 25 and Ra = 580.4 will be interpreted below.

The complete results for the Bénard–Marangoni problem with Pr = 1 are presented in figures 3 and 4. The curves expressing the critical Marangoni number Ma^c versus the critical

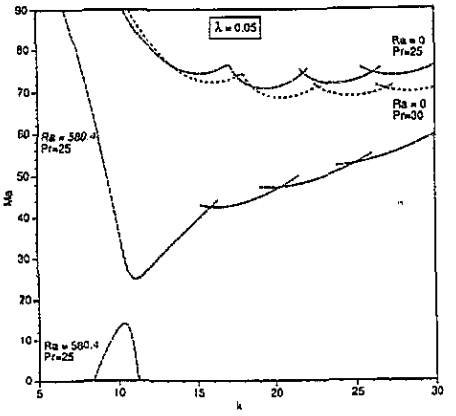

Figure 2. Neutral oscillatory curves for $\lambda = 0.05$. The results for $Ra = 580.4$ and $Pr = 25$ exhibit two distinct branches, one of them with a negative concavity.

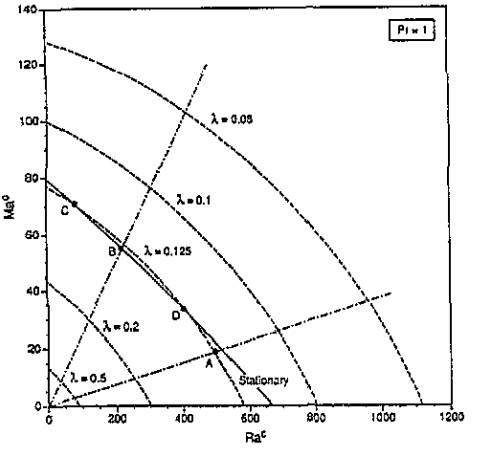

Figure 3. Critical Ma^c–Ra^c curves for $Pr = 1$, $0.08 \leqslant \lambda \leqslant 0.5$.

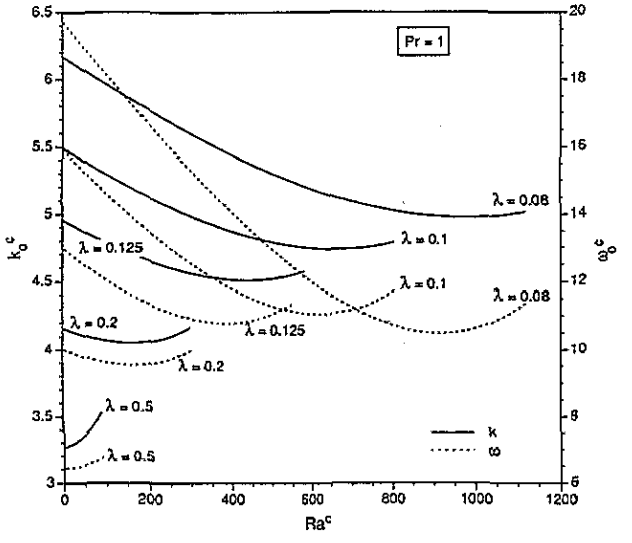

Figure 4. Critical wave-numbers and critical frequencies at $Pr = 1$ for various λ values. These results correspond to the curves presented in figure 3; k curves are represented by full curves, ω curves by broken curves.

Rayleigh number Ra^c corresponding to different values of the relaxation time λ are given in figure 3. The broken curves generalize Nield's result [7] obtained for a Newtonian fluid and represented by the solid line. According to Nield, the critical Marangoni and Rayleigh numbers for stationary instability in a Newtonian fluid are located on an approximate straight line given by

$$Ra^c/Ra_0^c + Ma^c/Ma_0^c \simeq 1$$

where Ra_0^c and Ma_0^c are the critical values of Ra and Ma corresponding to absence of surface-tension effects and absence of gravity respectively.

It is instructive to represent on this graph the evolution of the physical control parameter, namely the temperature difference ΔT between the lower and upper surfaces. According to the very definitions of the Marangoni and Rayleigh numbers, one has

$$\mathrm{Ma} = [(\partial\xi/\partial T)/\alpha g d^2]\mathrm{Ra}$$

from which it follows that for a given fluid and a given layer depth d the Ma and Ra values are aligned on a straight line passing through the origin. For a given fluid, the slope of this line is representative of the thickness of the layer: the line OA corresponds to a 'thick' layer (large d and Ra/Ma values), OB to a 'thin' layer (small d and Ra/Ma values). When ΔT is increased, one moves along the straight line, say OA, up to crossing the 'Nield's curves' describing the onset of convection: the crossing point A gives the critical ΔT^c value. In this picture, it is seen that when the relaxation time λ is increased, the system becomes more and more unstable. For λ smaller (larger) than some critical value, instability is stationary (oscillatory); for rather small λ, instability is stationary as for Newtonian fluids.

Consider in particular the curve corresponding to $\lambda = 0.125$. For that portion of broken curve lying below Nield's full curve (say point A), it must be understood that for the corresponding values of Ra, Ma, Pr and λ the instability occurs in the form of oscillations. In contrast, if the broken curve lies above the full curve, the instability is stationary. The situations described by the portion of the curve located above the full curve CD may however be interesting in experiments with imposed wave-numbers. The crossing of the broken curve and the solid curve (points C and D) describes an instability taking the form of a competition between a stationary mode and an oscillatory mode and is referred to as a point of codimension two. This situation has also been encountered in Newtonian fluids with a deformable upper surface [30]. Let us also notice that the curvature of the broken curves indicates that the coupling between the gravity and thermocapillarity effects is no longer quasi-linear as in stationary convection. The critical wave-number k_o^c and the critical frequency ω_o^c (indices o and c stand for 'oscillatory' and 'critical' respectively) for the oscillatory instabilities are represented in figure 4 as functions of the critical Rayleigh number. Clearly, the critical wave-numbers and the critical frequencies decrease when the relaxation time grows.

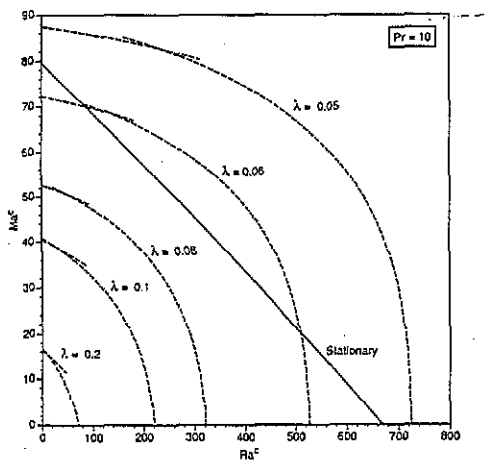

Figure 5. Critical Ma^c–Ra^c curves for Pr = 10 with λ varying between 0.2 and 0.5. Each overstable curve is formed by the reunion of two branches.

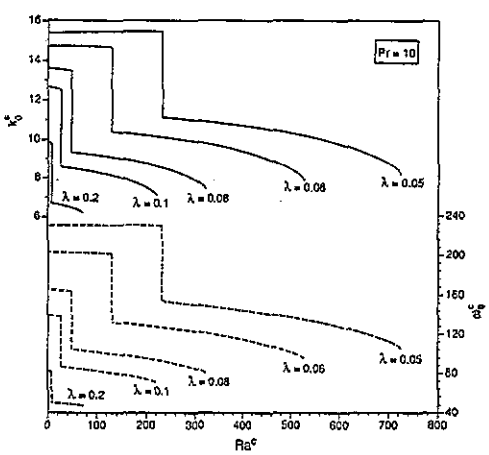

Figure 6. Critical wave-numbers and critical frequencies at Pr = 10 for various λ values. These results correspond to the curves presented in figure 5.

The situation for Pr = 10 is described in figures 5 and 6. The new feature is the appearance of a discontinuity in the slope of the broken curves (see figure 5). In connection

with these breaks, one observes discontinuities in the critical wave-numbers and the critical frequencies (see figure 6). At these transition points, one has a competition between two oscillatory modes with different wave-numbers and frequencies. This competition is not typical of viscoelastic fluids but appears also in Newtonian fluids with a deformable surface [30]. The origin of this behaviour may be found in the fact that, by increasing Ra, the 'height' of the different local minima of the neutral curve $Ma(k)$ are displaced with respect to each other so that the lowest minimum may jump from one critical k^c to another. More precisely, as seen in figure 2, when Ra is increased from 0 to 580.4, the second local minimum which is the lowest one at $Ra = 0$ decreases more slowly than the first one. So for high Ra values the first minimum becomes the lowest and thus determines the appearance of oscillatory convection. The break in the slope of the Nield curve occurs when the two minima have the same value. From an experimental point of view, it is interesting to notice that such discontinuities can easily be observed by using fluid layers of different thicknesses.

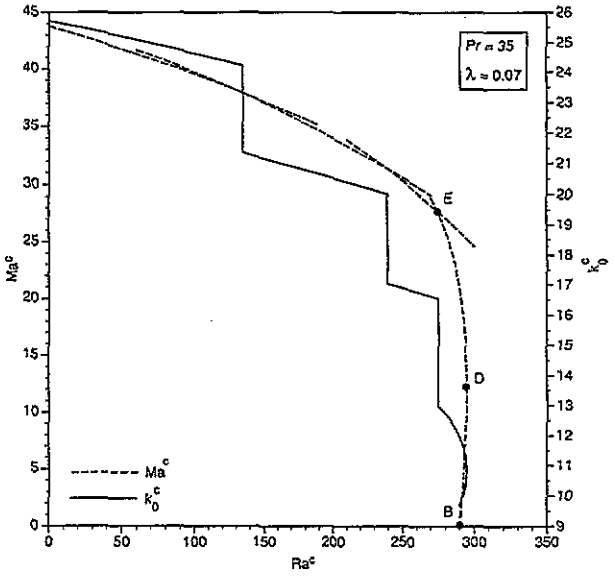

Figure 7. Critical Ma^c–Ra^c curve and corresponding critical wave-number k_0^c at $Pr = 35$ and $\lambda = 0.07$.

If the Prandtl number becomes larger, the number of discontinuities in the Ra^c–Ma^c and Ra^c–k_0^c planes increases (see figure 7 for $Pr = 35$). Another interesting result observed for rather large values of Pr is the appearance of a region BDE where the critical Rayleigh number is quasi-independent of the critical Marangoni number. A detailed examination of the results even shows that for rather small Ma, the slope of the Ma versus Ra curve between points B and D becomes positive. This means that in this range of values of the parameters, the Marangoni effect—which is usually thought of as destabilizing—reinforces the stability of the liquid layer. Generally, for a fixed value of Ra ($< Ra^B$), the system becomes unstable when Ma reaches a given value. For $Ra^B \leqslant Ra \leqslant Ra^D$, the system is stable for Marangoni numbers between a mimimum and a maximum value. Of course, due to the extremely steep slope of the stability curve, the stabilization effect is practically very weak. Going back to the representation of the marginal curves of figure 2, this effect is detected by the appearance of a second branch with negative concavity. The positive slope of the stability curve Ma versus Ra corresponds to the (positive) maxima of this second branch. A similar unusual result has also been displayed in a paper [31] by Davis and Homsy who showed that surface deflection—which is usually thought of as destabilizing—may also increase the

stability for a predominantly buoyancy-driven convection.

For high Pr values and pure Marangoni convection, we have observed that the various local minima of the neutral curves are very close to each other so that the corresponding modes are actually in competition.

5. Summary and final comments

We briefly summarize the main results which were obtained in terms of their dependence with respect to the various parameters.

We first recall that stationary instability curves $\mathrm{Ma}(k)$ depend only on the Rayleigh number and not on Pr or λ. In contrast, the overstability neutral curves are functions of the three parameters Ra, Pr and λ.

By increasing the relaxation time λ, the system becomes more and more unstable while the critical wave-number and the critical frequency decrease. It is also interesting to notice that for values of λ lower (greater) than some critical value, the instability is always stationary (oscillatory), whatever the value of the thickness (i.e. whatever the ratio Ra/Ma). For very small relaxation times, one recovers the results corresponding to a Newtonian fluid, as expected.

When Pr becomes greater and greater, the system becomes more and more unstable since the critical Marangoni and Rayleigh numbers decrease. Moreover, the lowest minimum of the neutral curves is displaced towards local minima located more on the right of the picture, at least for small Rayleigh numbers, which means an increase of the critical wave number. The critical frequency also grows with Pr. The increase of the Rayleigh number is generally accompanied by a decrease of the critical Marangoni number from which it follows that the Marangoni effect plays a destabilizing role. However, this behaviour is not always true in viscoelastic fluids where, as observed in figure 7, the Marangoni effect may reinforce stability in some range of variations of the various parameters. Moreover, at high Prandtl numbers, one has observed discontinuities in the critical wave-number and the critical frequency. These discontinuities are due to the fact that, when Ra is increased, the local minima of the neutral curves $\mathrm{Ma}(k)$ corresponding to high k values decrease more slowly than those corresponding to small k. As a consequence, the lowest minimum jumps from right to left towards smaller k values and the critical wave-number generally decreases with increasing Ra. In particular, for purely gravity driven convection ($\mathrm{Ma} = 0$), it was found that criticality corresponds always to the first local minimum of $\mathrm{Ma}(k)$.

In summary, the objective of the present work was to examine the Bénard–Marangoni instability in a thin Maxwell viscoelastic fluid layer. A linear analysis was carried out. The results have been interpreted in terms of the two relevant parameters, namely the Prandtl number Pr and the relaxation time λ appearing in the Maxwell equation. The present study completes earlier works [21–27] where one single motor of instability—either gravity or thermocapillarity—was considered.

Such an instability analysis is also interesting as it allows us, after measuring the critical temperature difference, to determine indirectly the rheological coefficients of the fluid, such as viscosity, heat conductivity and relaxation time, and to compare the values with the results of direct experimental measurements techniques which generally require a higher degree of refinement.

As observed by other authors, one important feature of thermoconvection in a viscoelastic fluid is the appearance of an oscillatory instability. As shown by Getachew and Rosenblat [26], this kind of oscillatory instability can be exhibited experimentally in

very thin layers in a microgravity environment. The present work provides the theoretical framework for studying thermocapillary instabilities in earth laboratories. Experimental confirmations would be desirable.

Acknowledgments

This text presents research results of the Belgian Interuniversity Poles of Attraction (PAI 21) initiated by the Belgian State, Prime Minister's Office, Science Policy Programming. The scientific responsibility is assumed by its authors. Two of us (G Lebon and M Grmela) wish also to express their gratitude for support from the Accords Culturels Communauté Française de Belgique—Québec under contract 04/12/1PP2-015-S.

References

[1] Bénard H 1900 *Rev. Gen. Sci. Pure Appl.* **11** 1261
[2] Chandrasekhar S 1961 *Hydrodynamic and Hydromagnetic Stability* (Oxford: Clarendon)
[3] Drazin P G and Reid W H 1981 *Hydrodynamic Stability* (Cambridge: Cambridge University Press)
[4] Platten J K and Legros J C 1984 *Convection in Liquids* (Berlin: Springer)
[5] Lebon G and Perez-Garcia C 1980 *Bull. Classe Sci. Acad. R. Belg.* **64** 520
[6] Pearson J R A 1958 *J. Fluid Mech.* **4** 489
[7] Nield D A 1964 *J. Fluid Mech.* **19** 341
[8] Normand C, Pomeau Y and Velarde M 1977 *Rev. Mod. Phys.* **49** 581
[9] Busse F H 1978 *Rep. Prog. Phys.* **41** 1929
[10] Pellew A and Southwell R V 1940 *Proc. R. Soc.* A **176** 312
[11] Scanlon J W and Segel L A 1967 *J. Fluid Mech.* **30** 149
[12] Cloot A and Lebon G 1984 *J. Fluid Mech.* **145** 447
[13] Vidal A and Acrivos A 1966 *Phys. Fluids* **9** 615
[14] Segel L A *1965 J. Fluid Mech.* **21** 345
[15] Segel L A 1965 *J. Fluid Mech.* **21** 359
[16] Davis S H 1987 *Ann. Rev. Fluid Mech.* **19** 403
[17] Bird R B, Armstrong R C and Hassager O 1987 *Dynamics of Polymeric Liquids* 2nd edn, vol I (New York: Wiley)
[18] Tanner R I 1985 *Engineering Rheology* (Oxford: Oxford University Press)
[19] Barnes H A, Hutton J F and Walters K 1989 *An Introduction to Rheology* (Amsterdam: Elsevier)
[20] Joseph D D 1990 *Fluid Dynamics of Viscoelastic Liquids* (New York: Springer)
[21] Eltayeb I A 1977 *Proc. R. Soc.* A **358** 161
[22] Rosenblat S 1986 *J. Non-Newtonian Fluid Mech.* **21** 20
[23] Martínez-Mardones J and Pérez-García C 1990 *J. Phys.: Condens. Matter* **2** 1281
[24] Vest C M and Arpaci V S 1969 *J. Fluid Mech.* **36** 613
[25] Sokolov M and Tanner R I 1972 *J. Phys. Fluids* **15** 534
[26] Getachew D and Rosenblat S 1985 *Acta Mechanica* **55** 137
[27] Lebon G and Cloot A 1988 *J. Non-Newtonian Fluid Mech.* **28** 61
[28] Vidal A and Acrivos A 1966 *Phys. Fluids* **9** 615
[29] Takashima M 1970 *J. Phys. Soc. Japan* **20** 810
[30] Pérez-García C and Carneiro G 1991 *Phys. Fluids* A **3** 292
[31] Davis S H and Homsy G M 1980 *J. Fluid Mech.* **98** 527